Research Article

Filip Vujović, Aleksandar Valjarević*, Josep Vila-Subirós, Ante Šiljeg, and Tin Lukić

Geospatial modeling of wildfire susceptibility on a national scale in Montenegro: A comparative evaluation of F-AHP and FR methodologies

https://doi.org/10.1515/geo-2022-0694
received May 29, 2024; accepted August 16, 2024

Abstract: Wildfires pose a significant ecological, environmental, and socioeconomic challenge in southeastern Europe. The preservation of wildlands is not only essential but also a foremost priority for Montenegro, a country recognized as the world's first ecological state. Consequently, the development of optimal methodologies and models is of paramount importance to enhance fire protection measures. With this objective in mind, this study strives to create a wildfire susceptibility model on a national scale for Montenegro. The study employed seven natural and anthropogenic causative criteria: vegetation type; aspect; slope; elevation; climate classification; distance from road; and population. The modeling process integrates both natural and anthropogenic causal criteria, employing the Fuzzy Analytic Hierarchy Process (F-AHP) and Frequency Ratio (FR) within geoinformatics environment. The outcomes of the F-AHP model reveal that 72.84% of the total area is categorized as having high to very high susceptibility. Conversely, based on the FR model, only 29.07% of the area falls within these susceptibility levels. In terms of validation, the area under curvature values indicates good performance of the F-AHP model. In contrast, the FR model demonstrates poor performance. These novel findings, pertaining to Montenegro at a national scale, offer valuable insights for preemptive wildfire safeguarding efforts. Moreover, the methodologies employed, with necessary modifications, hold potential for application in geographically diverse regions.

Keywords: wildfire susceptibility, F-AHP, FR, Montenegro, wildfire management, geoinformatic, GIS

*** Corresponding author: Aleksandar Valjarević,** Faculty of Geography, University of Belgrade, Studentski Trg 3/III, 11000, Belgrade, Serbia; Faculty of Education, University of East Sarajevo, Semberskih ratara 1E, Bjeljina, Bosnia and Herzegovina, e-mail: aleksandar.valjarevic@gef.bg.ac.rs
Filip Vujović: Department of Geography, Faculty of Philosophy, University of Montenegro, Danila Bojovića bb, 81400, Nikšić, Montenegro; Environmental Protection Agency of Montenegro, IV Proleterske 19, 81000, Podgorica, Montenegro, e-mail: vujovicfilip@hotmail.com
Josep Vila-Subirós: Department of Geography, Socio-Environmental Change Research Group (SAMBI), Environmental Institute, University of Girona, Plaça Ferrater Mora 1, 17004, Girona, Spain, e-mail: josep.vila@udg.edu
Ante Šiljeg: Department of Geography, University of Zadar, Trg Kneza Višeslava 9, 23000, Zadar, Croatia, e-mail: asiljeg@unizd.hr
Tin Lukić: Department of Geography, Tourism and Hotel Management, Faculty of Sciences, University of Novi Sad, Trg Dositeja Obradovića 3, 21000, Novi Sad, Serbia, e-mail: tin.lukic@dgt.uns.ac.rs

1 Introduction

Uncontrolled wildfires rage in a natural setting, with vegetation serving as the predominant and primary source of fuel [1]. Characterized as significant natural disasters, these events escalate the magnitude of destruction and play a role in the devastation of forests, bushes, grasslands, and other wildland areas. Annually, hundreds of millions of hectares of these vegetation areas are globally obliterated through this phenomenon [2]. Since these wildfires are a global phenomenon, they represent a constant threat to the environment, ecological, and socio-economic systems in which they occur [3,4].

In 2020, despite increased readiness levels among European Union countries, approximately 340,000 hectares were burned across Europe. By October 29, 2021, a report from the Joint Research Centre indicated that wildfires had affected about 0.5 million hectares, with forests accounting for 61% of the impacted areas. A quarter of the affected zones were located within "Natura 2000," the EU's biodiversity reserve. These fires have spread across southern, central, and northern Europe, with Romania experiencing the most severe impact, followed by Portugal, Spain, and Italy. Looking ahead, there is an expected increase in wildfire risk in Southeast Europe and the Mediterranean due to climate change and human influence, underscoring the critical need for conserving wildland areas [5,6]. According to the data

from the Forestry Administration, between 2010 and 2020, Montenegro experienced 1,001 major wildfires, resulting in the destruction of 50139.33 ha of forests and damage or destruction of over 900,000 m^3 of timber. In the record-breaking year of 2017, fires engulfed 21215.86 ha of forested areas [7].

In this regard, geoinformation technologies take center stage as a dependable approach for crafting methods and models for proactive wildfire prevention. Geoinformation technologies present a broad spectrum of innovative, cost-effective, and efficient solutions for sustainable geospatial management [8,9]. These technologies have proven highly valuable across various applications, including environmental planning and management [10,11], responses to natural disasters [12–14], addressing climate changes [15], managing hydrology and water resources [16], as well as in agriculture and forestry [17,18].

The utilization of low- and medium-resolution geospatial data from European and global databases (i.e., MODIS, Copernicus, WorldClim, and OpenStreetMap) has been applied across various geographic regions worldwide to derive criteria for modeling wildfire susceptibility, hazard, vulnerability, and risk [19–21]. In extensive areas where the creation of distinct groups of natural and anthropogenic criteria is necessary, very high-resolution commercial satellite images from WorldView 2 and 3 satellites are employed [22]. Additionally, aerial photogrammetric data in high and very high resolution collected by Unmanned Aerial Vehicles (UAV) and Light Detection and Ranging (LIDAR) technology have also been applied in developing criteria for modeling wildfire risk [23–25].

GIS multi-criteria analysis (GIS-MCDA) utilizing Analytical Hierarchy Process (AHP) [19,23,24,26–32] and Fuzzy Analytical Hierarchy Process (F-AHP) [31–37] approaches are frequently employed in numerous global studies to model wildfire vulnerability, susceptibility, hazard, and risk. In addition to these methodologies, various studies employ different approaches such as Frequency Ratio (FR) [36–39], Shannon Entropy (SE) [39–41], Weight of Evidence (WoE) [42,43], Statistical Index (SI) [43,44], Fuzzy Logic [45,46], Logistic regression (LR) [47,48] and among Machine Learning methods [49–55] are commonly utilized.

Machine Learning methods [49–55] are increasingly employed with a harmonized approach. Indeed, the choice between methodologies for assessing wildfire susceptibility often hinges on specific needs and preferences. Following validation, the superiority of machine learning methods in performance is often attributed to their ability to capture complex patterns and relationships within data. This can result in more accurate predictions compared to traditional methodologies [52,54]. However, the simplicity of statistical processing and ease of interpretation of results offered by other methodologies, such as AHP, F-AHP, and FR, is one of the advantages compared to machine learning methods. Despite their slightly weaker performance in some cases, the straightforwardness of these methodologies can contribute to a better understanding and implementation of wildfire risk management strategies.

There isn't much research or previous studies addressing this issue in Montenegro. Pioneering research across Montenegro was conducted by Hysa and Spalevic [56]. This study developed a wildfire spread capacity index using European and global low- to medium-resolution data, revealing a high wildfire spread capacity in Montenegro. Vujović [57] carried out GIS modeling for wildfire mapping using open low- to medium-resolution data in his master's thesis. The results showed that the research area of Budva predominantly falls into categories of high and very high fire hazards, with the developed model demonstrating good performance after validation. Božović et al. [58] emphasized the significance and potential of the project titled "Building Capacity for Disaster Risk Reduction through the National Forest Fire Information System," implemented by the Ministry of Internal Affairs of Montenegro – Directorate for Protection and Rescue and the Japan International Cooperation Agency since 2021. The project aims to base its activities on the already developed Macedonian information system, which assesses fire hazards and risk using existing national and low-resolution European data. The project plans to develop networks of meteorological stations to assess the meteorological index at the onset of fires. Since the project is still in the implementation phase, specific results are not yet available. Nikolić et al. [32] assessed wildfire susceptibility in Budva, a coastal municipality in Montenegro, and Rožaje, a northern municipality with varying climates. Similar to previous research, low- to medium-resolution data were used here to obtain natural and anthropogenic criteria. Modeling results indicated that over 80% of the territory in Budva and Rožaje falls into categories of high and very high susceptibility. In this GIS-MCDA-based study, both the AHP and F-AHP models exhibit similar performance.

With all this in mind, the objective of this study is to construct a pioneering wildfire susceptibility model on a national scale for Montenegro. Previous studies have primarily relied on AHP and FR methods. This study, however, is the first to compare F-AHP and FR. The modeling procedure incorporates natural and anthropogenic criteria, utilizing the F-AHP and FR methodologies within a geoinformatics framework. The study extensively scrutinizes both methodological approaches during the validation phase, subjecting them to comprehensive evaluation and analysis.

2 Materials and methods

2.1 Study area

Montenegro, situated in southeastern Europe on the Balkan Peninsula, spans from latitudes 41°52′ to 43°32′N and longitudes 18°26′ to 20°21′E (Figure 1). It encompasses an area of 13,883 km^2 and is home to a population of approximately 620,000 inhabitants. It has a coastline of 293.5 km along the Adriatic Sea [59].

The distribution of terrain can be categorized as follows: up to 200 m covering 10% of the area, between 200 and 1,000 m covering 33%, between 1,000 and 1,500 m covering 39%, and above 1,500 m covering 18% [60]. It is noteworthy that over 60% of the terrain consists of carbonate formations, where the predominant relief type is karst. The landscape is characterized by diverse landforms, including sandy and rocky coasts, karst fields, plateaus, canyons, and high mountains exhibiting periglacial characteristics within a relatively compact area [61].

According to Köppen's classification, two climate types are observed in the reference climate period [62]: warm temperate (*C*) and cold temperate (*D*). The warm temperate climate predominates in lower elevation regions, while in the higher mountainous areas within Montenegro, particularly above 1,000 m, the climate shifts to the cold temperate type.

Montenegro can be geographically divided into three distinct regions: Coastal, Central, and Northern Montenegro. Administratively, the country is divided into 25 municipalities [59]. The Coastal region, with its characteristic appearance, exhibits all the typical features of Mediterranean areas. Being the smallest by area (11.6% of the total area), this region, which essentially coincides with the geomorphologically defined and distinct area of the Coastal, encompasses the municipalities of Herceg Novi, Kotor, Tivat, Budva, Bar, and Ulcinj. The majority of tourism activity is concentrated within this region, making it the primary generator of tourist traffic in Montenegro.

The Central region, the most pronounced lowland area of Montenegro, is surrounded by arid limestone surfaces. Besides the well-known natural resources (bauxite reserves and hydroelectric potential), its significant natural potential lies in the complexes of agricultural land. This region encompasses 35.5% of the total area, and in terms of geomorphology, it includes defined and distinct areas such as the Valleys of central Montenegro, the Plateau of deep karst, and the southern part of the Central high plateaus,

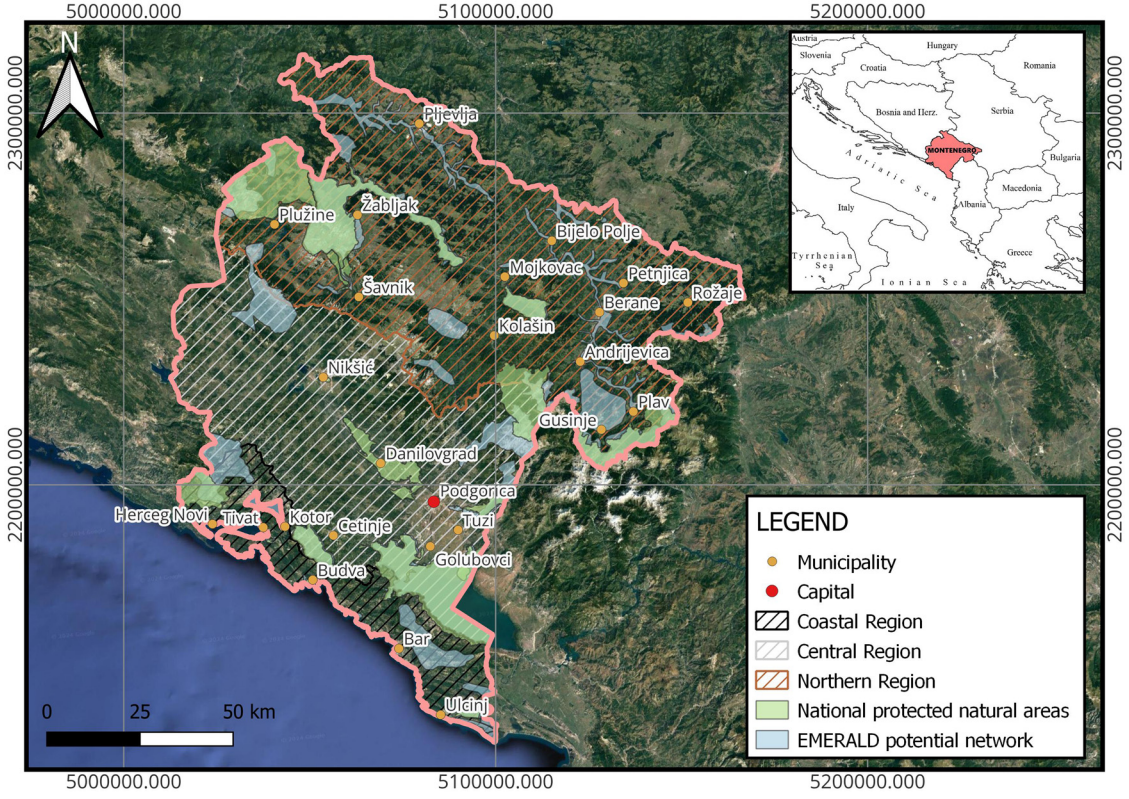

Figure 1: Location map of Montenegro.

encompassing the municipalities of Podgorica, Tuzi, Zeta, Danilovgrad, Nikšić, and Cetinje. The Northern region is an extremely high mountainous part of the territory, intersected by river valleys and, in many of its parts, resembles the characteristic relief forms of Alpine landscapes. Arable agricultural areas located along river valleys and slopes, vast pastures, extensive complexes of high-quality forests (beech and coniferous), significant reserves of coal, lead, and zinc, considerable hydroelectric potential, and very favorable conditions for the development of mountain and spa tourism in most areas represent the most significant natural resources and potentials of this region. The northern region occupies over half of the total area of Montenegro (52.9% of the total area) and is primarily composed of areas defined as the Central high plateaus and the Northeastern Montenegro region, with administrative centers in Kolašin, Mojkovac, Žabljak, Savnik, Plužine, Pljevlja, Bijelo Polje, Petnjica, Berane, Andrijevica, Plav, Gusinje, and Rožaje.

In 1991, Montenegro made a declaration stating its status as an ecological country. By embedding this declaration into its Constitution, Montenegro became the first country in the world to officially proclaim itself as such. The distinctive combination of geological background, climate, terrain, hydrography, and land cover has led to the emergence of two biogeographical regions (Alpine and Mediterranean) in Montenegro's geographic space. These regions exhibit exceptional biodiversity, highlighted by Montenegro's 3,250 plant species and a floristic diversity index (S/A1) of 0.837. This positions Montenegro as one of the "hot spots" of biodiversity in the Mediterranean region and one of the 153 globally significant centers of floristic diversity [60].

According to the results of the First National Forest Inventory (NFI) [63], Montenegro is characterized by a high level of forest coverage, at 59.5% (826,782 ha). Forest land occupies 9.9% (137,480 ha). Together, forests and forest land make up 69.4% of Montenegro's territory. High forests encompass 51.1% of the overall forest area, with low-growth forests occupying 48.9%. State-owned forests represent 52.3%, whereas private forests account for 47.7% of the total forested land. Within Montenegro, deciduous trees prevail, covering 76.2% of the forested area. Conifers exhibit a notably greater volume and growth rate within the total volume compared to deciduous trees. The share of conifers in the total volume is 40.2%. Approximately 38.7% of accessible forests and 7.5% of accessible forestland are designated as potential Natura 2000 Annex I habitats. A substantial portion of these areas is legally protected, with 5.2% of forests located within national parks and 14.6% falling within Emerald zone territories.

Between 2005 and 2015, Montenegro experienced approximately 800 significant wildfires, resulting in the destruction or impairment of over 18,000 ha of forest and more than 800,000 m^3 of wood. The particularly severe year was 2012, with fires impacting 7% of the forested area. However, the most devastating fire season occurred in 2017, witnessing the registration of 124 wildfires exceeding 30 ha. These fires affected a total area of 51,661 ha [7].

2.2 Input data for causative criteria

To apply the F-AHP and FR methods, it was essential to choose relevant causative criteria for the analysis. These criteria were determined by considering a blend of factors specific to the area under study area, a review of relevant literature, and input from experts at the Environmental Protection Agency of Montenegro. The study employed seven natural and anthropogenic causative criteria: (C1) vegetation type; (C2) aspect; (C3) slope; (C4) elevation; (C5) climate classification; (C6) distance from road; and (C7) population. Wildfire susceptibility modeling excludes artificial areas and water bodies based on the Boolean logic concept, which has values of 0. The criteria were derived from open geospatial data and national databases, which underwent transformation into a 500-meter grid and were subsequently reprojected into the ETRS89-extended/LAEA Europe (EPSG: 3035) projection. Table 1 provides details on the criteria, data sources, resolutions, and formats utilized in modeling.

2.2.1 Criterion vegetation type

The structure of the wildlands plays a crucial role in wildfires, serving as a primary consideration in susceptibility assessments due to its significant impact on both the onset and behavior of fires [64]. Combustible materials such as trees, leaves, and grass act as suitable fuels which can initiate fires. Typically, coniferous species exhibit higher burning potential compared to deciduous species, attributed to the presence of gum and resins in their cambium and leaves. However, variability in flammability exists even among different species within the same category of trees. An additional factor that has an impact on susceptibility is the age of the trees. Grasslands and shrublands have a lower availability of fuel than woods, although they are extremely dry. As a result, wildfire intensity in these areas is generally low, yet flames spread quickly. The susceptibility to wildfires is significantly affected by abandoned agricultural areas that have ceased cultivation [65]. Vegetation types and their characteristics were given based on the CORINE Land Cover 2018 database (Figure 2a).

Table 1: Causative criteria with format and source

Code	Criteria	Data	Source
C1	Vegetation type	ESRI Shapefile	https://land.copernicus.eu/pan-european/corine-land-cover/clc2018 (accessed on 10 March 2024)
C2	Aspect	GeoTIFF (25 m)	https://land.copernicus.eu/imagery-in-situ/eu-dem/eu-dem-v1.1 (accessed on 10 March 2024)
C3	Slope	GeoTIFF (25 m)	https://land.copernicus.eu/imagery-in-situ/eu-dem/eu-dem-v1.1 (accessed on 10 March 2024)
C4	Elevation	GeoTIFF (25 m)	https://land.copernicus.eu/imagery-in-situ/eu-dem/eu-dem-v1.1 (accessed on 10 March 2024)
C5	Climate classification	ESRI Shapefile	https://canupub.me/knjiga/atlas-klime-crne-gore/ (accessed on 10 March 2024)
C6	Distance from road	ESRI Shapefile	https://www.geofabrik.de/ (accessed on 10 March 2024)
C7	Population	ESRI Shapefile	http://www.geoportal.co.me/ (accessed on 10 March 2024)

The aim of this database is to collect, coordinate, and provide consistent information on natural resources and the environment in Europe. So far, CLC status layers have been created for 1990, 2000, 2006, 2012, and 2018, and the nomenclature for these layers consists of three levels: the first level indicates the main land cover categories, the second level is for use at scales of 1:500,000 and 1:1,000,000, and the third level is for use at a scale of 1:100,000. As for the status layers, the accuracy of the satellite images used ranges from 10 to 50 m. The geometric accuracy of the CLC is 100 m. The minimum mapping unit is 25 ha for polygons, and the minimum line thickness for linear entities is 100 m. Thematic accuracy is ≥85% [66].

2.2.2 Topographic group of criteria: Aspect, slope, and elevation

The primary topographical elements affecting wildfire occurrence and spread are aspect (Figure 2b), slope (Figure 2c), and elevation (Figure 2d) [24]. The aspect or orientation of the slope determines the level of solar radiation received depending on the side of the world it faces. Slope is a key factor affecting wildfire spread. It is generally known that wildfire spreads faster uphill than downhill. This phenomenon of expansion on sloping terrain is triggered by warm air rising up the slope, further drying out the combustible materials. It is important to point out that the slope can reduce the influence of the wind, but it can also increase it. This solar radiation significantly impacts the moisture content in the fuel, consequently influencing the spread of the fire. With increasing elevation, air temperature decreases while humidity rises, correlating with precipitation levels and temperature variations, ultimately impacting wildfire susceptibility [67].

Analysis of the topographic criteria was conducted utilizing the functionalities of QGIS software, with the topographic data sourced from the European Digital Elevation Model (EU-DEM) model. The EU-DEM, crafted by the European Environmental Protection Agency (EPA), covers the lands of 27 European Union (EU) member states and 6 partner nations [68]. This amalgamated dataset, named EU-DEM, predominantly utilizes information from SRTM DEM and ASTER GDEM, complemented by openly available Russian topographic maps for regions beyond 60°N. The model exhibits moderate resolution, characterized by a geospatial resolution of 25 m. The projected root mean square error (RMSE) for the standard vertical precision of the revised edition (EU-DEM v1.1) stands at roughly 7 m [69].

2.2.3 Criterion climate classification

The climate plays a crucial role in both the ignition and escalation of wildfires. Its influence extends to every aspect affecting the susceptibility of wildfires. This interaction underscores the significance of climate in shaping the conditions conducive to wildfire occurrence and spread, highlighting its pivotal role in wildfire management and prevention efforts. Nikolić et al. [32] demonstrated in their research that identical or analogous criteria can be applied across various climate zones in Montenegro. To examine the connection between wildfire occurrences and climatic elements, a digitized map illustrating climate zones based on the Köppen classification system (Figure 2e), outlined by Burić et al. [62]. Köppen's formula relies on numerical values for temperature and precipitation, along with defining characteristic thresholds for these variables, which delineate between different climate types based on their impacts on plant life, animal habitats, and human activities [70].

2.2.4 Anthropogenic group criteria: Distance from road and population

The group of anthropogenic causal criteria used includes distance from road (Figure 3a) and population (Figure 3b). These two criteria serve a dual purpose: they act as

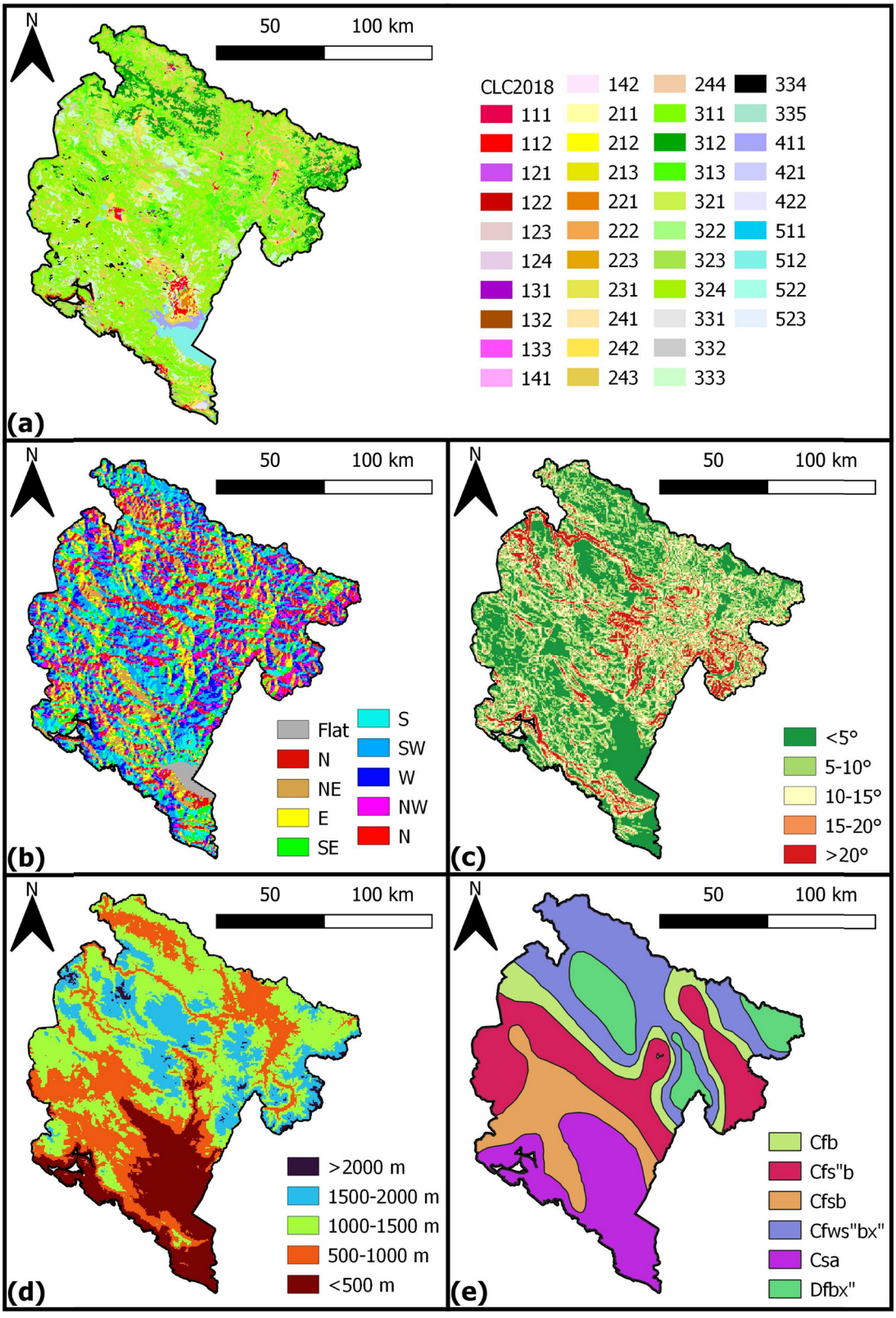

Figure 2: Natural causal criteria. (a) vegetation type; (b) aspect; (c) slope; (d) elevation; (e) climate classification.

mitigating factors in reducing susceptibility to wildfires by establishing fire barriers and escape routes, while simultaneously serving as potential contributors to heightened vulnerability due to human activities, tourism, and recreational endeavors in wildland areas [26]. Euclidean analysis was utilized in QGIS to determine distance from road, with data sourced from the OpenStreetMap database serving as input for this analysis. Data on the human population were obtained based on statistical circles. Statistical circles represent the smallest geospatial units within a unified statistical territorial registry, covering the entire territory of Montenegro. These are permanent units, with boundaries that can only be changed under exceptional circumstances and according to established criteria. These data are compiled by the Statistical Office of Montenegro – MONSTAT and the Administration for Cadastre and State Property of Montenegro [71].

2.3 Correlation analysis

Correlation analysis was conducted between all causal criteria. The "corrplot" package in RStudio was employed for this purpose. This package calculates correlations based on the Pearson correlation method by default. The resulting correlogram offers both visual and numerical insights into the correlation coefficient of each pair of criteria. In the correlogram, larger and darker blue circles indicate a stronger positive correlation between criteria, while larger and darker red circles signify a greater inverse correlation between variables.

2.4 Historical wildfire data

For the scope of this study, geospatial subsets of Moderate Resolution Imaging Spectroradiometer (MODIS) historical wildfire locations within the borders of Montenegro for the period 2001–2022 were obtained from the FIRMS geoportal (https://firms.modaps.eosdis.nasa.gov/(accessed March 10, 2024)), utilizing the archive download tool for the standard product MCD14ML. Each point represents the center of a 1 km pixel identified by the MODIS MOD14/MYD algorithm for thermal anomalies and wildfires [72]. Only locations with a confidence level exceeding 80% were chosen. In building the wildfire susceptibility model, historical wildfire data were randomly divided into 70% (1,116 points) for training and 30% (478 points) for testing (Figure 4).

2.5 F-AHP method

F-AHP is a methodology within GIS-MCDA that focuses on key decision-making criteria. Integrating multi-criteria analysis with GIS results in GIS-MCDA is a process that involves converting and merging geospatial data to generate valuable new information for decision-making purposes. The GIS-MCDA stands as one of the prevailing methods for susceptibility modeling, finding utility across diverse scientific domains [73]. The GIS-MCDA procedure utilized in this study for modeling wildfire susceptibility consists of three sequential steps (Figure 5): standardizing causal criteria values, assigning criteria weights, and

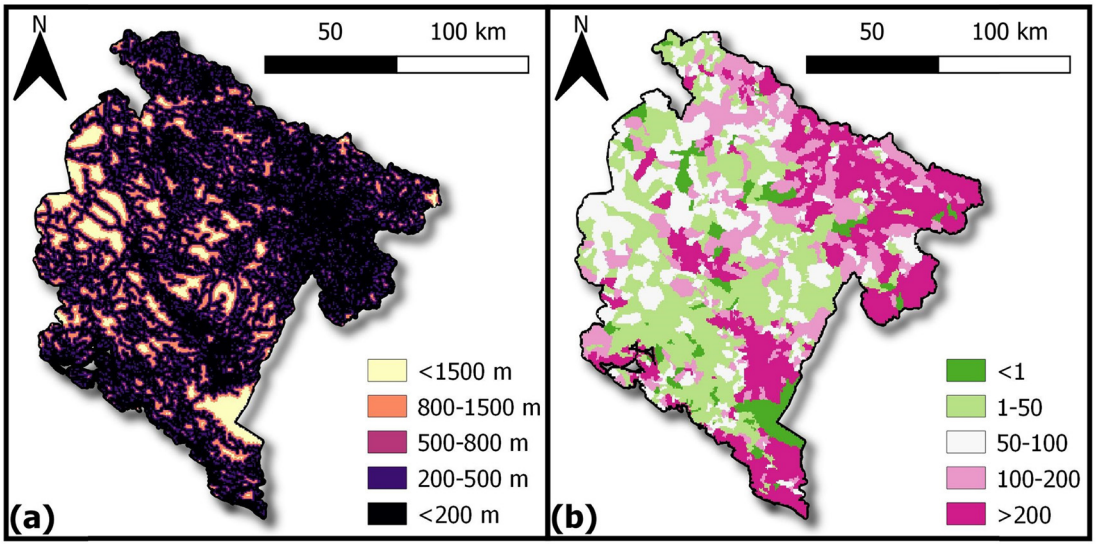

Figure 3: Anthropogenic causal criteria: (a) distance from road; (b) population.

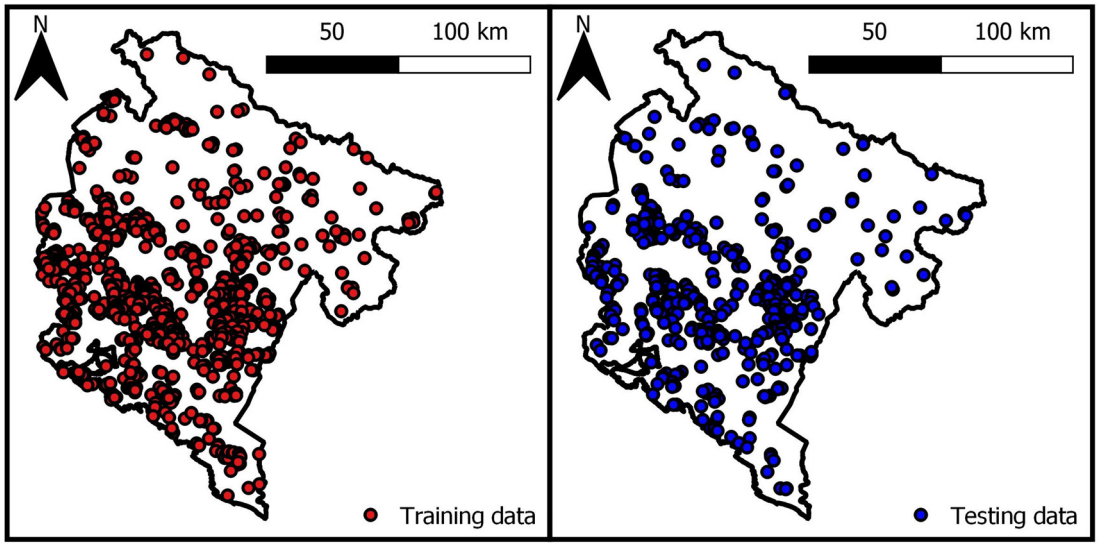

Figure 4: Training and testing MODIS locations.

analyzing results (Combination of Standardized Values and Weight of Criteria). The entire GIS-based methodological procedure was carried out in QGIS 3.28.3 software (https://www.qgis.org/en/site/forusers/download.html (accessed 10 March 2024)).

The standardization and weighting of criteria values followed a similar approach to the selection of causal criteria. This process involved considering a combination of area-specific factors, reviewing relevant literature, and consulting with experts from the Environmental Protection Agency of Montenegro. The normalization of the values for all criteria was carried out according to the evaluation method in a numerical interval from 1 (very low) to 5 (very high), with the ranges of values for each class being determined separately.

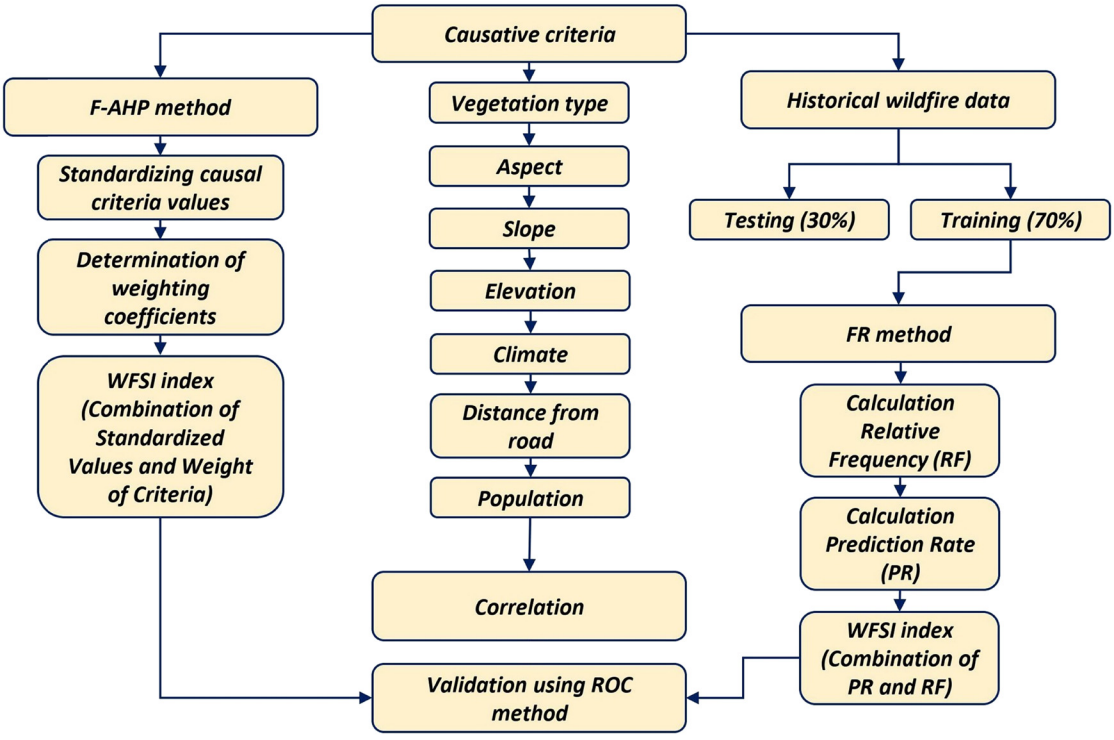

Figure 5: Flow chart illustrating the procedural steps of the F-AHP and FR method.

Weighting coefficients for the causal criteria regarding wildfire susceptibility importance are determined using the F-AHP methodology. Numerous methodological approaches incorporate fuzzy elements within pairwise comparison matrices. For this analysis, we chose Ramík's approach [74], which is implemented in online software, available at (https://fuzzyahp.holecekp.eu/(accessed 12 March 2024)) [75]. This approach is built upon pairwise comparison of triangular fuzzy elements. Such a matrix $\tilde{A}$ has the following form [74]:

$$\tilde{A} = \begin{bmatrix} (a_{11}^L, a_{11}^M, a_{11}^U) & \dots & (a_{1n}^L, a_{1n}^M, a_{1n}^U) \\ \vdots & \ddots & \vdots \\ (a_{n1}^L, a_{n1}^M, a_{n1}^U) & \dots & (a_{nn}^L, a_{nn}^M, a_{nn}^U) \end{bmatrix}, \quad (1)$$

where for all $i, j = 1, \dots, n$

- $a_{ij}^L, a_{ij}^M, a_{ij}^U$ are real numbers such that $1/\sigma \le a_{ij}^L \le a_{ij}^M \le a_{ij}^U \le \sigma$ for a chosen fixed $\sigma > 1$.
- $\tilde{a}_{ij} = (a_{ij}^L, a_{ij}^M, a_{ij}^U)$ implies that $\tilde{a}_{ji} = \left(\frac{1}{a_{ij}^U}, \frac{1}{a_{ij}^M}, \frac{1}{a_{ij}^L}\right)$. (reciprocity)

Besides the introduction of the fuzzy triangular elements, another difference compared to the classical Saaty's AHP is that the preference intensities provided by the expert are not limited to the interval $\left[\frac{1}{9}, 9\right]$, but can be taken more general form $\left[\frac{1}{\sigma}, \sigma\right]$ for a chosen value $\sigma > 1$.

Fuzzy weights are obtained through the following procedure [74]:

$$w_k^L = C_{\min} \cdot \frac{(\prod_{j=1}^n a_{kj}^L)^{1/n}}{\sum_{i=1}^n (\prod_{j=1}^n a_{ij}^M)^{1/n}}, \quad \text{where}$$

$$C_{\min} = \min_{i=1,\dots,n} \left\{ \frac{(\prod_{j=1}^n a_{ij}^M)^{1/n}}{(\prod_{j=1}^n a_{ij}^L)^{1/n}} \right\}$$

$$w_k^M = \frac{(\prod_{j=1}^n a_{kj}^M)^{1/n}}{\sum_{i=1}^n (\prod_{j=1}^n a_{ij}^M)^{1/n}}, \quad (2)$$

$$w_k^U = C_{\max} \cdot \frac{(\prod_{j=1}^n a_{kj}^U)^{\frac{1}{n}}}{\sum_{i=1}^n (\prod_{j=1}^n a_{ij}^M)^{\frac{1}{n}}}, \quad \text{where}$$

$$C_{\max} = \max_{i=1,\dots,n} \left\{ \frac{(\prod_{j=1}^n a_{ij}^M)^{\frac{1}{n}}}{(\prod_{j=1}^n a_{ij}^U)^{\frac{1}{n}}} \right\}.$$

The following index was used to assess matrix consistency [74]:

$$\mathrm{NI}_n^\sigma(\tilde{A}) = \gamma_n^\sigma \cdot \max_{i,j} \left\{ \max \left\{ \left| \frac{w_i^L}{w_j^U} - a_{ij}^L \right|, \left| \frac{w_i^M}{w_j^M} - a_{ij}^M \right|, \left| \frac{w_i^U}{w_j^L} - a_{ij}^U \right| \right\} \right\}, \quad (3)$$

where

$$\gamma_n^\sigma = \begin{cases} \dfrac{1}{\max\left\{\sigma - \sigma^{(2-2n/n)}, \sigma^2\left(\left(\frac{2}{n}\right)^{2/(n-2)} - \left(\frac{2}{n}\right)^{n/(n-2)}\right)\right\}} & \text{if } \sigma < \left(\frac{n}{2}\right)^{n/(n-2)} \\ \dfrac{1}{\max\{\sigma - \sigma^{(2-2n/n)}, \sigma^{(2n-2/n)} - \sigma\}} & \text{otherwise.} \end{cases} \quad (4)$$

The numerical values assigned to the index range between 0 and 1, with 0 indicating complete consistency of the matrix.

The modeling results were produced by F-AHP methods using the weighted linear combination method at 500 m resolution. In this method, standardized values and weighting coefficients are combined, and the analysis is conducted using Raster Calculator tool, applying the given equation [76]:

$$\mathrm{WFSI} = \sum w_i \times x_i \times \prod E. \quad (5)$$

WFSI is the wildfire susceptibility index in the case of this model, w_i is the weighting coefficient of the criteria, and x_i is the value of the standardized criteria. The exclusion area ($\prod E$) is calculated using Boolean logic principles and holds a value of 0. The WFSI values align with the evaluation range of criteria 1 to 5, with scores categorized as very low (1), low (2), moderate (3), high (4), and very high (5) susceptibility.

2.6 FR method

The FR method is based on the concept of the favorability function [77]. FR represents the ratio between historical wildfire occurrences and their geospatial correlation with causal criteria contributing to the event [78]. Training samples from the MODIS satellite were used to perform this analysis. As with the F-AHP method, the entire GIS-based procedure is implemented in QGIS software (Figure 5).

The FR values for each class within the criteria were obtained using the following equation [77]:

$$\mathrm{FR} = \frac{N_{\mathrm{pix}}(\mathrm{LX}_i)/\sum_{i=1}^m N_{\mathrm{pix}}(\mathrm{LX}_i)}{N_{\mathrm{pix}}(X_j)/\sum_{j=1}^n N_{\mathrm{pix}}(X_j)}, \quad (6)$$

where FR is the frequency ratio of class i of parameter j. $N_{\mathrm{pix}}(\mathrm{LX}_i)$ is the number of pixels with wildfires within class i of parameter criteria X. $N_{\mathrm{pix}}(X_j)$ is the number of pixels within parameter criterion X_j. m is the number of classes in the parameter criterion X_i, and n is the number of causal criteria in the study.

The RF were then standardized to the range of probability values [0, 1] as the relative frequency in the next phase (RF). The equation is shown in the continuation [77]:

$$\mathrm{RF} = \frac{\mathrm{FR}_{ij}}{\sum_{i=1}^m \mathrm{FR}_{ij}}. \quad (7)$$

Even after equalization, the RF frequency still suffers from the limitation of treating all conditioning elements equally. The prediction rate (PR) was calculated to evaluate each conditioning component using the training dataset, according to the following equation [77]:

$$\mathrm{PR} = \frac{(\mathrm{RF}_{\max} - \mathrm{RF}_{\min})}{(\mathrm{RF}_{\max} - \mathrm{RF}_{\min})_{\min}}. \tag{8}$$

The WFSI is calculated according to the following equation:

$$\mathrm{WFSI} = \sum_{i=1}^{n} (\mathrm{PR} \times \mathrm{RF}) \times \prod E, \tag{9}$$

where WFSI stands for the Wildfire Susceptibility Index, while PR represents the prediction rate for the criterion, and RF denotes the relative frequency for the criterion. Top of Form ($\prod E$) presents exclusion areas determined through the application of Boolean logic principles, with a corresponding value of 0. The WFSI values were divided into five susceptibility classes via the Natural Breaks (Jenks) technique, distinguished as very low, low, moderate, high, and very high [44].

2.7 Validation of employed methods

Validating the obtained results is a crucial stage in the modeling process as it enables the assessment of the relevance and validity of the developed F-AHP and FR models. For model validation, 30% of test samples were drawn from historical wildfire locations sourced from the MODIS satellite. The receiver operating characteristic curve (ROC) in LibreOffice Calc was utilized as a validation technique. The ROC curve is widely used in geospatial modeling. With the ROC curve, it is possible to display the false positive fraction in relation to the true positive for all values used to generate the modeling results. The ROC curve graph depicts specificity on the *x*-axis and sensitivity on the *y*-axis. Additionally, for validation purposes, an automatically calculated area under curvature (AUC) was created at ROC. The AUC values indicate the success and accuracy of a given model with respect to the reference data, with excellent (AUC = 0.9–1), good (AUC = 0.8–0.9), fair (AUC = 0.7–0.8), poor (AUC = 0.6–0.7), and failed models (AUC = 0.5–0.6) [79].

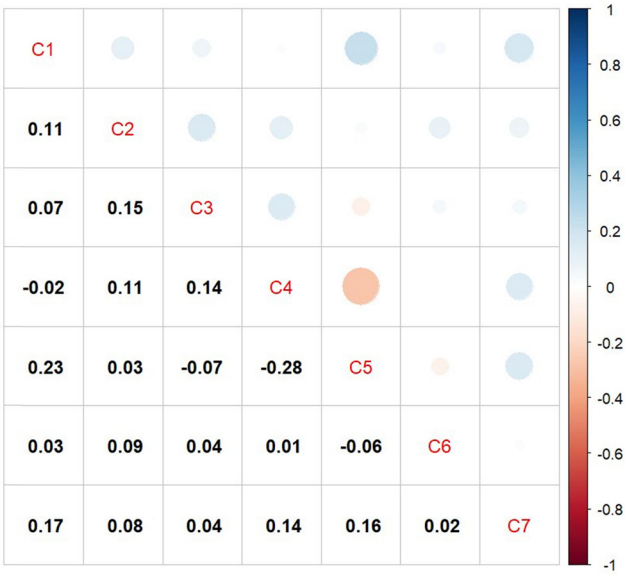

Figure 6: Correlogram for causal criteria.

3 Results

3.1 Correlation between causal criteria

Figure 6 illustrates a correlogram, presenting visual and numerical indications of the correlation coefficients among the causal criteria. Larger circles and darker blue shades signify stronger positive correlations, while larger circles and darker red shades indicate stronger inverse correlations among the causal criteria. As the results show, the highest negative correlation value (−0.28) was found between elevation and climate classification. However, the highest value of positive correlation (0.23) was determined between vegetation type and climate classification. The correlation observed among other causal criteria similarly suggests a lack of robustness or substantial influence between the selected causal criteria.

3.2 Wildfire modeling by F-AHP

Causal criteria were standardized on a numerical scale ranging from 1 (very low) to 5 (very high), as shown in Table 2. The weighting coefficients for these criteria, determined through the F-AHP procedure within the online software solution, are illustrated in Figure 7. The matrix inconsistency, as measured by the NI value, is deemed acceptable. The primary criterion with the highest weight coefficient is vegetation type, followed by climate classification, distance of road, population density, aspect, slope, and elevation, respectively. The results of modeling conducted via the F-AHP procedure, which was employed in calculating the WFSI, are outlined in Table 3. Furthermore, Figure 8 complements the geospatial distribution illustrated in the overview map. As per

Table 2: Standardization of criteria

	Intensity of importance				
Code for causal criteria	**Very low (1)**	**Low (2)**	**Moderate (3)**	**High (4)**	**Very high (5)**
Vegetation type (C1)*	332, 333	331, 334, 411	211, 212, 221, 222, 223, 231, 241, 242, 243, 311	313, 321, 322, 324	312, 323
Aspect (C2)	N	NE, NW	E, W	SE, Flat	S, SW
Slope (C3)	<5°	5–10°	10–15°	15–20°	>20°
Elevation (C4)	>2,000	1,500–2,000 m	1,000–1,500 m	500–1,000 m	<500 m
Climate classification (C5)	Dfbx”	Cfws“bx”, Cfb	Cfs”b	Cfsb	Csa
Distance from road (C6)	>1,500 m	800–1,500 m	500–800 m	200–500 m	<200 m
Population (C7)	<1	1–50	50–100	100–200	>200

*CLC 2018 classes. Available online: https://land.copernicus.eu/user-corner/technical library/corine-land-cover-nomenclature guidelines/docs/pdf/CLC2018_Nomenclature_illustrated_guide_20190510.pdf (accessed March 10, 2024)).

the F-AHP model's findings, a substantial 72.84% of the total area demonstrates high to very high susceptibility. Within this distribution, the moderate category holds a significant share of 20.80%, highlighting its considerable presence. In contrast, the low category accounts for just 2.53%, indicating its minimal representation. Excluded areas occupy 3.83%.

In assessing wildfire susceptibility across three distinct regions, the Coastal region emerges as particularly

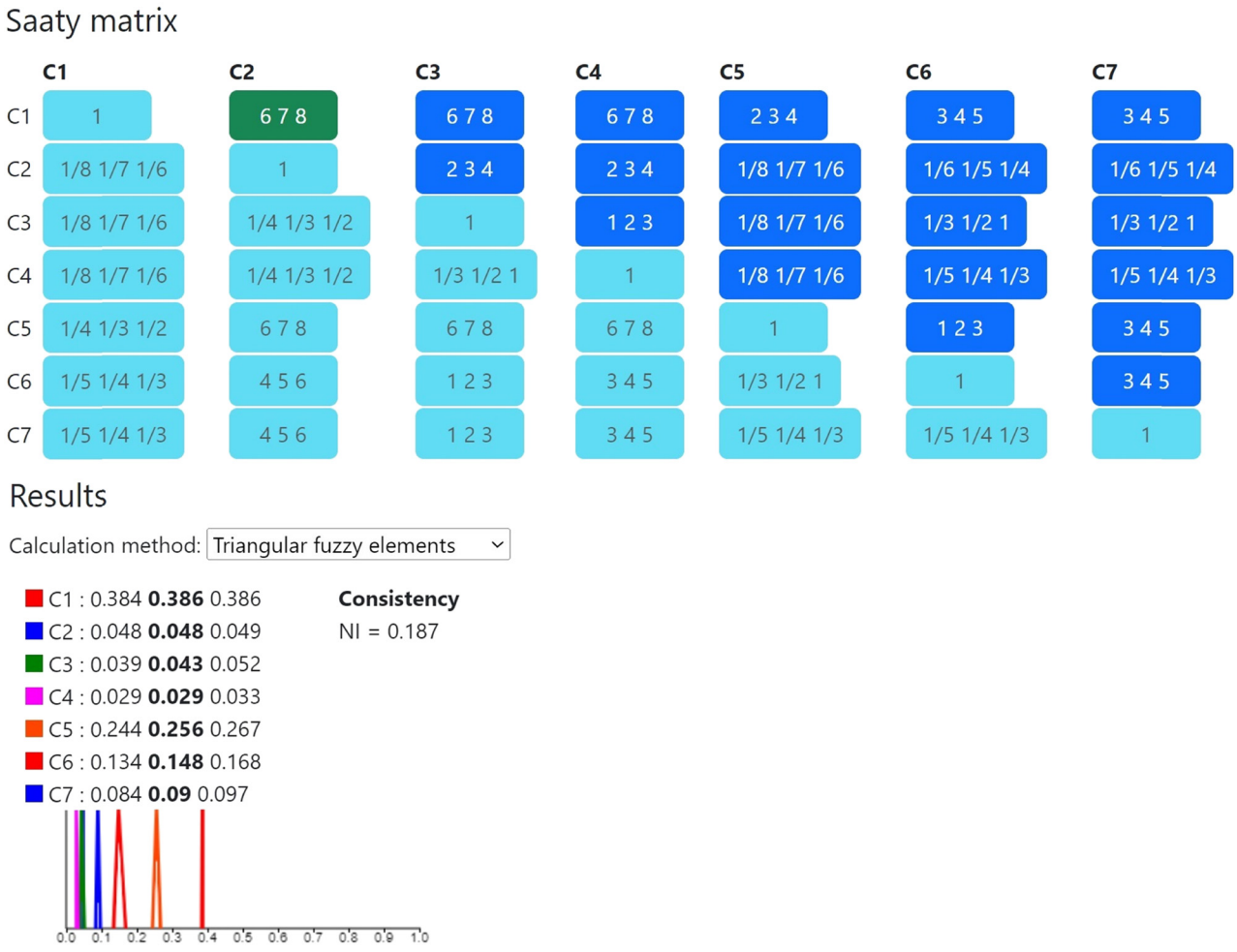

Figure 7: F-AHP weight coefficients for causal criteria.

Table 3: Percentage of the area in different areas of interest according to the F-AHP model % of area

Area of interest	Excluded areas	Very low	Low	Moderate	High	Very high
The whole area	3.83	—	2.53	20.80	66.08	6.76
Coastal region	6.32	—	0.03	10.11	50.05	33.48
Central region	7.73	—	1.38	18.51	65.59	6.79
Northern region	0.56	—	3.85	24.57	69.60	1.41
National protected areas	14.64	—	3.65	22.87	51.88	6.95
EMERALD	9.37	—	4.60	23.26	58.60	4.17

susceptible, with over 50.05% of its area classified as having a high susceptibility and a further 33.48% categorized as very high. This indicates a significant portion of land, amounting to approximately 83.53% in total. The Central region also demonstrates concerning levels of susceptibility, with over 72.38% of its area falling within the high to very high categories. In the Northern region, the combined area of high and very high wildfire susceptibility categories is precisely 71.01%. In the Coastal region, moderate susceptibility occupies 10.11% of the area, while low susceptibility is minimal at 0.03%. Similarly, in the Central region, moderate susceptibility covers 18.51% of the area, with low susceptibility constituting 1.38%. Meanwhile, in the Northern region, moderate susceptibility encompasses 24.57% of the area, while low susceptibility covers 3.85%.

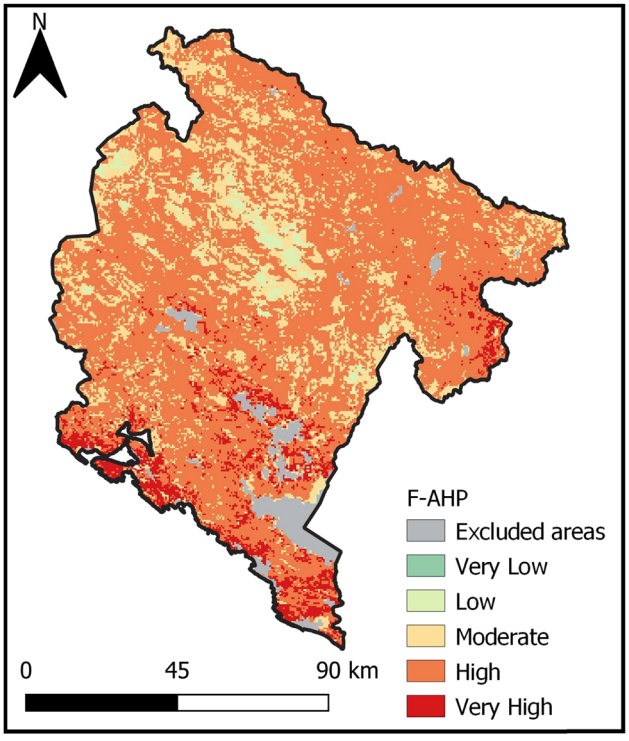

Figure 8: Spatial display of the F-AHP model by susceptibility categories.

The Coastal region makes up 6.32% of the areas excluded, while the Central region comprises 7.73%. In contrast, the Northern region accounts for a mere 0.56%.

In the context of nationally protected natural areas and wildfire susceptibility, the provided data illustrates varying levels of susceptibility across different categories. Nationally protected natural areas include strict nature reserves, national parks, special nature reserves, nature parks, natural monuments, and landscapes of exceptional characteristics. The analyzed terrestrial nationally protected natural areas occupy about 13% of the total area of Montenegro. As for the excluded areas, which are mostly occupied by water bodies, they make up 14.64% of the total area. Meanwhile, low susceptibility areas cover 3.65%, moderate susceptibility areas cover 22.87%, high susceptibility areas cover 51.88%, and very high susceptibility areas cover 6.95% of the total area.

Montenegro has designated approximately 18% of its territory to the European Network of Areas of Special Conservation Interest (EMERALD). The provided model indicates that excluded areas, which typically encompass water bodies, constitute 9.37% of the total area. Low susceptibility areas cover 4.60%, moderate susceptibility areas cover 23.26%, and high susceptibility areas, including both high and very high categories, cover the majority at 62.77% of the total area.

3.3 Wildfire modeling by FR

Table 4 displays FR values for causal criteria derived from the training sample for historical wildfire locations. Out of natural and anthropogenic causal criteria used for FR susceptibility modeling, the criterion of distance from roads among anthropogenic criteria exhibits the highest prediction ratio (PR) value. It is followed by climate classification, elevation, population density, vegetation type, slope, and aspect, respectively. The modeling results obtained through the FR procedure, utilized to derive the WFSI, are presented in Table 5. As with the F-AHP model, the excluded areas occupy

Table 4: Frequency ratio (FR) and prediction rate (PR) for causal criteria

Code for causal criteria	Class	Number of pixels in class	Percentage of domain (PD)	Number of wildfire pixels	Percentage of wildfire (PW)	Frequency ratio (FR)	Prediction rate (PR)
C1	111	8	0.01	0	0.00	0.00	
	112	801	1.44	0	0.00	0.00	
	121	79	0.14	0	0.00	0.00	
	122	8	0.01	0	0.00	0.00	
	123	7	0.01	0	0.00	0.00	
	124	17	0.03	0	0.00	0.00	
	131	65	0.12	0	0.00	0.00	
	132	24	0.04	0	0.00	0.00	
	133	26	0.05	0	0.00	0.00	
	141	16	0.03	0	0.00	0.00	
	142	42	0.08	0	0.00	0.00	
	211	33	0.06	0	0.00	0.00	
	221	117	0.21	7	0.63	2.98	
	222	5	0.01	0	0.00	0.00	
	223	20	0.04	0	0.00	0.00	
	231	1,082	1.95	14	1.25	0.64	
	241	5	0.01	0	0.00	0.00	
	242	1,165	2.10	12	1.08	0.51	
	243	6,554	11.80	64	5.73	0.49	
	311	14,670	26.41	351	31.45	1.19	
	312	3,958	7.12	31	2.78	0.39	
	313	4,198	7.56	73	6.54	0.87	
	321	4,095	7.37	54	4.84	0.66	
	322	20	0.04	0	0.00	0.00	
	323	441	0.79	13	1.16	1.47	
	324	11,670	21.01	472	42.29	2.01	
	331	63	0.11	0	0.00	0.00	
	332	663	1.19	12	1.08	0.90	
	333	3,819	6.87	0	0.00	0.00	
	334	298	0.54	0	0.00	0.00	
	411	442	0.80	12	1.08	1.35	
	421	6	0.01	0	0.00	0.00	
	422	62	0.11	0	0.00	0.00	
	511	33	0.06	0	0.00	0.00	
	512	1,026	1.85	1	0.09	0.05	
	522	1	0.00	0	0.00	0.00	
	523	13	0.02	0	0.00	0.00	
	Sum	**55,552**	**100.00**	**1,116**	**100.00**	**13.51**	**1.54**
C2	Flat	638	1.15	0	0.00	0.00	
	North	6,649	11.97	113	10.13	0.85	
	Northeast	7,957	14.32	181	16.22	1.13	
	East	6,213	11.18	129	11.56	1.03	
	Southeast	5,404	9.73	117	10.48	1.08	
	South	7,594	13.67	160	14.34	1.05	
	Southwest	9,379	16.88	215	19.27	1.14	
	West	6,368	11.46	101	9.05	0.79	
	Northwest	5,350	9.63	100	8.96	0.93	
	Sum	**55,552**		**1,116**		**8.00**	**1.00**
C3	0–5	18,791	33.83	299	26.79	0.79	
	5–10	18,242	32.84	333	29.84	0.91	
	15–20	10,087	18.16	228	20.43	1.13	
	20–25	4,861	8.75	132	11.83	1.35	
	>25	3,571	6.43	124	11.11	1.73	
	Sum	**55,552**	**100.00**	**1,116**	**100.00**	**5.91**	**1.11**

(Continued)

Table 4: *Continued*

Code for causal criteria	Class	Number of pixels in class	Percentage of domain (PD)	Number of wildfire pixels	Percentage of wildfire (PW)	Frequency ratio (FR)	Prediction rate (PR)
C4	0–500	8,904	16.03	173	15.50	0.97	
	500–1,000	15,020	27.04	360	32.26	1.19	
	1,000–1,500	21,706	39.07	476	42.65	1.09	
	1,500–2,000	9,381	16.89	107	9.59	0.57	
	>2,500	541	0.97	0	0.00	0.00	
	Sum	**55,552**	**100.00**	**1,116**	**100.00**	**3.82**	**2.18**
C5	Csa	10,349	18.63	228	20.43	1.10	
	Cfsb	7,926	14.27	346	31.00	2.17	
	Cfs“b	12,965	23.34	396	35.48	1.52	
	Cfb	5,766	10.38	60	5.38	0.52	
	Cfws“bx”	12,753	22.96	34	3.05	0.13	
	Dfbx”	5,793	10.43	52	4.66	0.45	
	Sum	**55,552**	**100.00**	**1,116**	**100.00**	**5.89**	**2.42**
C6	0–500	30,706	55.27	379	33.96	0.61	
	500–1,000	13,740	24.73	290	25.99	1.05	
	1,000–1,500	5,363	9.65	95	8.51	0.88	
	1,500–2,000	2,937	5.29	233	20.88	3.95	
	>2,500	2,806	5.05	119	10.66	2.11	
	Sum	**55,552**	**100.00**	**1,116**	**100.00**	**8.61**	**2.71**
C7	<1	3,135	5.64	41	3.67	0.65	
	1–50	15,745	28.34	484	43.37	1.53	
	50–100	11,627	20.93	246	22.04	1.05	
	100–200	10,890	19.60	207	18.55	0.95	
	>200	14,155	25.48	138	12.37	0.49	
	Sum	**55,552**	**100.00**	**1,116**	**100.00**	**4.67**	**1.57**

Bold values are important to distinguish difference between causal criteria in FR methodology.

3.83% of the area. Furthermore, Figure 9 complements the geospatial distribution illustrated in the overview map. Based on the FR model, the very high susceptibility category shows the smallest percentage representation at just 8.61%, whereas the high category boasts 20.46%. The moderate category comprises 25.79% of the representation, slightly behind the low category, which accounts for 25.87%. Meanwhile, the very low category accounts for 15.44%.

Starting with the Coastal Region, excluded areas account for 6.32% of the total area. Here, the distribution across categories is as follows: low (0.03%), moderate (10.11%), high (50.05%), and very high (33.48%). Moving on to the Central Region, excluded areas make up 7.73% of the overall total area. The distribution across categories within this region stands at very low (8.44%), low (13.43%), moderate (29.20%), high (24.97%), and very high (16.22%). Shifting focus to the Northern Region, excluded areas represent a mere 0.56% of the total. Within this region, the breakdown shows very low (17.63%), low (35.91%), moderate (24.14%), high (18.13%), and very high (3.63%).

As for the nationally protected natural areas, the excluded areas are mostly occupied by water bodies,

Table 5: Percentage of the area in different areas of interest according to the FR model % of area

Area of interest	Excluded areas	Very low	Low	Moderate	High	Very high
The whole area	3.83	15.44	25.87	25.79	20.46	8.61
Coastal region	6.32	29.43	19.52	21.98	16.05	6.70
Central region	7.73	8.44	13.43	29.20	24.97	16.22
Northern region	0.56	17.63	35.91	24.14	18.13	3.63
National protected areas	14.64	17.41	26.27	19.00	17.91	4.77
EMERALD	9.37	17.53	25.72	22.59	17.92	6.86

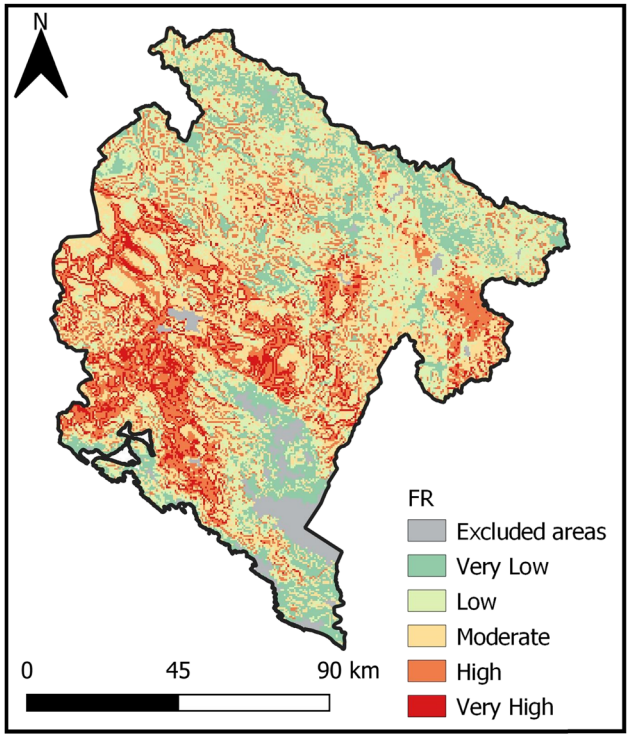

Figure 9: Spatial display of the FR model by susceptibility categories.

making up 14.64% of the total area. Within this segment, the breakdown across categories is as follows: very low (17.41%), low (26.27%), moderate (19.00%), high (17.91%), and very high (4.77%).

The resulting model in the EMERALD potential areas shows that the excluded areas, which usually include water bodies, make up 9.37% of the total area. The distribution across categories within this region stands at very low (17.53%), low (25.72%), moderate (22.59%), high (17.92%), and very high (6.86%).

3.4 Validation

For validation purposes, 30% of the testing dataset, equivalent to 478 historical wildfire locations, was employed. The validation results shown on the ROC curve for the F-AHP and FR methodological approaches are shown in Figure 10. Specifically, the AUC values derived from the ROC curve serve as a measure of each model's predictive accuracy. In this context, a higher AUC value indicates superior model performance. After testing, the F-AHP model demonstrated good performance in validation with an AUC value of 0.82, while the FR model showed poor performance with an AUC of 0.64. These findings underscore the effectiveness of the F-AHP approach in predicting wildfire susceptibility. The additional processed training samples used to construct the model display nearly identical values to the test samples (Figure 11).

4 Discussion

Wildfires pose a significant ecological, environmental, and socioeconomic challenge in southeastern Europe. The preservation of wildland is not only essential but also a foremost priority for Montenegro, a country recognized as the world's first ecological state. It's crucial to note that the assessment methods for wildfire risk can differ among

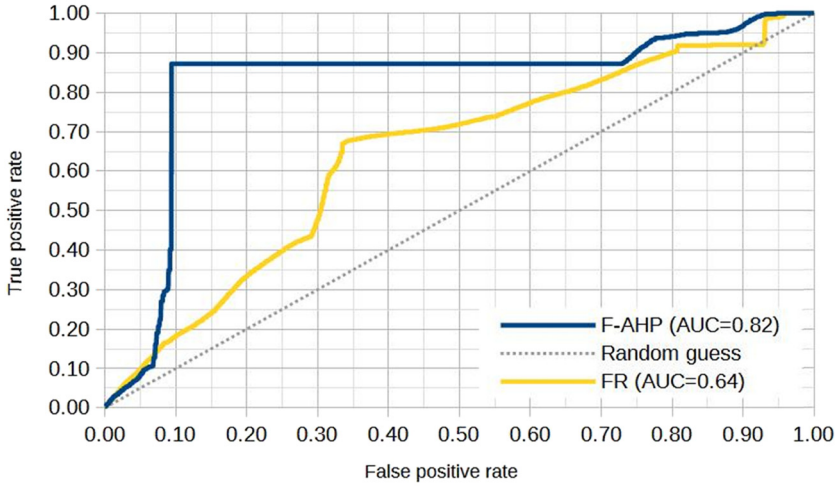

Figure 10: Results of the ROC curve analysis with AUC values for testing data.

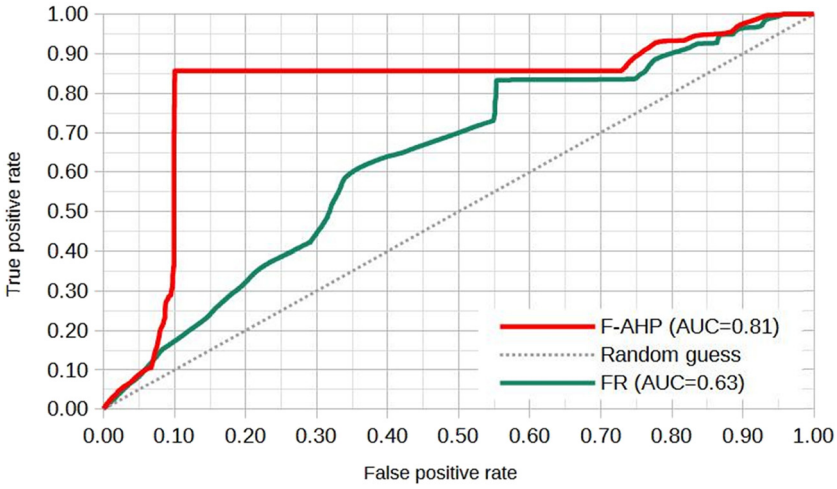

Figure 11: Results of the ROC curve analysis with AUC values for training data.

countries and research teams, resulting in diverse regional and national approaches that may not always be directly comparable. This variability is particularly relevant as wildfires frequently cross borders, impacting multiple countries simultaneously. Understandably, these divergent approaches emphasize the specificities of the respective regions of interest, with chosen methods being influenced by each country's unique characteristics [6]. In numerous instances documented in scientific and professional literature, when dealing with extensive geospatial coverage at medium and low resolutions, the complete implementation of risk assessment procedures becomes challenging. Instead, satisfactory outcomes are often achieved through the assessment of wildfire susceptibility. This susceptibility is defined as the static probability of wildfire in a given area, contingent on the essential terrain characteristics [55].

Carnicer et al. [80] explore how global warming is changing the relationships between wildfire weather and CO_2 emissions from wildfires in Europe, emphasizing the increased wildfire risk in Mediterranean countries, including Montenegro. Kreider et al. [81] argue that while fire suppression can be effective in the short term, it is not sustainable in the long term. They suggest that alternative land management strategies, such as controlled burning and the revival of agricultural and livestock activities, are necessary to prevent the accumulation of biomass that could fuel future mega-fires. Rouet-Leduc et al. [82] support this perspective by showing the positive impact of large herbivores on fire regimes and wildfire mitigation, advocating for their inclusion in land management policies.

Standards for determining weighting coefficients for various causal criteria, such as vegetative, topographical, climatic, and anthropogenic factors, frequently depend on expert opinions or static methodologies that utilize specific training samples [19,23–55]. By combining these approaches, researchers aim to establish a comprehensive and consistent framework that facilitates the understanding and analysis of these diverse causal criteria for differentiation. This integration not only enhances the reliability of the results but also supports more nuanced insights into how these factors interact and influence each other in various contexts [54].

In the study by Pradeep et al. [38], the AHP model demonstrated superior AUC performance compared to the FR model after validation. Conversely, Abdo et al. [37] found that the FR model slightly outperformed the AHP model, exhibiting somewhat higher AUC values. Additionally, Zeleke's master's thesis [83] emphasized that the AHP model outperforms the FR model. When comparing the AHP and F-AHP models, the F-AHP model consistently shows better performance than the AHP model, a finding supported by previous studies [31,32,84].

This study utilizes F-AHP and FR methods for geospatial modeling of wildfires, offering detailed insight into the susceptibility of various regions and protected natural areas in Montenegro to wildfire. Both approaches employ distinct causal criteria and weighting mechanisms to assess susceptibility, with F-AHP emphasizing vegetation type and climate classification as primary determinants, while FR prioritizes factors like distance from roads and elevation. In terms of susceptibility categorization, F-AHP identifies a substantial portion of Montenegro, as highly susceptible to wildfires, with over 72.84% of the total area falling into high to very high susceptibility categories. FR highlights a reduced proportion of areas exhibiting high and very high susceptibility, amounting to 29.07%, while displaying a more evenly distributed range across categories.

In comparing the findings of F-AHP and FR methodologies regarding wildfire susceptibility across Coastal, Central, and Northern regions, both approaches underscore significant concerns. F-AHP indicates that the Coastal region stands out as the most susceptible, with over 83.53% of its area classified as highly to very highly susceptible, followed by the Central and Northern regions at 72.38 and 71.01%, respectively. Conversely, FR analysis presents a more nuanced picture, with lower percentages of high to very high susceptibility across all regions – 22.75% in the Coastal, 41.20% in the Central, and 21.75% in the Northern region.

Similar to the regional level, in assessing wildfire susceptibility within nationally protected natural areas and the EMERALD potential network in Montenegro, both F-AHP and FR methodologies show discrepancies in the distribution across susceptibility categories, with F-AHP indicating a higher proportion of high and very high susceptibility areas compared to FR.

In Montenegro, the F-AHP method identifies a significant portion of nationally protected natural areas, with 51.88% categorized as highly susceptible and an additional 6.95% as very highly susceptible to wildfires. Similarly, within the EMERALD regions, the F-AHP method reveals a dominance of high and very high susceptibility categories, covering 62.77% of the total area. In contrast, the FR method suggests lower susceptibility levels, with 17.91% classified as high susceptibility and 4.77% as very high susceptibility within nationally protected natural areas. Similarly, in the EMERALD regions, the FR method indicates 17.92% falling into the high susceptibility category and 6.86% into the very high susceptibility category.

These differences underscore the importance of considering the nuances of each methodology's categorization approach when evaluating wildfire susceptibility. When considering validation results, F-AHP demonstrates good predictive accuracy, as indicated by its higher AUC value on the ROC curve compared to FR. This suggests that the F-AHP method is more effective in predicting wildfire susceptibility based on historical wildfire locations.

The limitations of utilizing low-resolution data and the subjective nature of F-AHP methods impact the obtained results, reducing accuracy in geospatial analyses like wildfire susceptibility modeling. Similarly, the FR method, though widely used, oversimplifies complex relationships between variables and relies heavily on the assumption of stationarity, potentially leading to biased results due to sensitivity to outliers and skewed data distributions. These drawbacks should be taken into account when employing these methods in geospatial analysis.

Overall, while both F-AHP and FR methodologies contribute valuable insights into wildfire susceptibility, F-AHP appears to offer a more robust and accurate predictive model, particularly in the context of Montenegro's landscape and environmental causal criteria. However, a comprehensive assessment necessitates a thorough exploration of the distinct strengths and limitations of each method, taking into consideration factors such as data availability to various geographical contexts, and their alignment with geoinfromation functionalities, including geospatial analysis, data integration, and visualization capabilities.

In future research, it would be beneficial to compare the F-AHP and FR approaches with machine learning methods. Additionally, incorporating additional causal criteria that have not been previously used could enhance the analysis and provide deeper insights into the outcomes. It would also be valuable to obtain historical fire data directly from emergency services and field sources. This comprehensive approach could lead to a more thorough understanding of the effectiveness of these methodologies.

5 Conclusions

A novel approach to geospatial modeling of wildfire susceptibility has been executed for the first time on a national scale in Montenegro within geoinformatics environment, leveraging F-AHP and FR methodologies. This pioneering endeavor marks a significant advancement in the field, providing a comprehensive assessment of wildfire susceptibility across the country. Nevertheless, following validation, the F-AHP method demonstrates significantly superior performance when contrasted with the FR approach. The comparison between F-AHP and FR methodologies reveals varying degrees of wildfire susceptibility across all regions. The F-AHP findings highlight significant concerns regarding wildfire susceptibility across all regions, with the coastal region emerging as the most susceptible, followed closely by the central and northern regions. Conversely, FR analysis presents a more nuanced picture, with lower percentages of high to very high susceptibility across all regions. The unique characteristics of each region, such as the tourism concentration in the Coastal, agricultural potential in the Central, and diverse natural resources in the Northern, further emphasize the need for tailored wildfire management strategies. The F-AHP method indicates that a significant proportion of nationally protected areas in Montenegro and the EMERALD areas are highly susceptible to wildfires, while the FR method suggests lower susceptibility levels. The abundant biodiversity and vast forested areas, comprising over 69% of Montenegro's land, render it highly susceptible to wildfires, particularly evident in its nationally protected areas and EMERALD zones,

as evidenced by the study's findings. This study has several limitations that may affect accuracy. The use of low-resolution data and the subjective nature of F-AHP reduce precision in wildfire susceptibility modeling. Additionally, the FR method oversimplifies relationships and relies on the assumption of stationarity, which can introduce bias. These novel findings, pertaining to Montenegro at a national scale, offer valuable insights for preemptive wildfire safeguarding efforts. Consequently, it can be inferred that Montenegro grapples with expansive areas at elevated susceptibility to wildfires, demanding immediate attention and robust mitigation measures to mitigate the potential for devastating wildfire outbreaks. Moreover, the methodologies employed, with necessary modifications, hold potential for application in geographically diverse regions.

Acknowledgments: The authors express their gratitude to the Environmental Protection Agency of Montenegro. The study was funded by the Ministry of Education, Science and Technological Development of the Republic of Serbia (Contract number 451–03–68/2022–14/200091).

Funding information: This research received no external funding that has supported the work.

Author contributions: Conceptualization, F.V., A.V., A.Š., J.V., and T.L.; methodology, F.V., T.L., J.V., A.V., and A.Š.; software, F.V. and A.V.; validation, A.Š. and F.V.; formal analysis, A.V., F.V., A.Š., T.L., and J.V; investigation, F.V., A.V., A.Š., J.V.; writing – original draft preparation, F.V., T.L., J.V., A.V., and A.Š.; writing – review and editing, F.V., A.V., A.Š., J.V., and T.L; visualization, F.V. and A.V.; supervision, T.L., A.V., J.V., F.V. and A.Š. All authors have read and agreed to the published version of the manuscript.

Conflict of interest: The authors state no conflict of interest.

References

[1] Leblon B, Bourgeau-Chavez L. Wildfire In: Bobrowsky PT, editor. Encyclopedia of Natural Hazards. Dordrecht: Springer; 2013. p. 1102–7. doi: 10.1007/978-1-4020-4399-4_31.

[2] Arora VK, Melton JR. Reduction in global area burned and wildfire emissions since 1930s enhances carbon uptake by land. Nat Commun. 2018;9(1):1326. doi: 10.1038/s41467-018-03838-0.

[3] Lukić T, Marić P, Hrnjak I, Gavrilov MB, Mladjan D, Zorn M, et al. Forest fire analysis and classification based on a Serbian case study. Acta Geograph Slovenica. 2017;57(1):51–63. doi: 10.3986/AGS.918.

[4] Kala CP. Environmental and socioeconomic impacts of forest fires: A call for multilateral cooperation and management interventions. Nat Hazards Res. 2023;3(2):286–94. doi: 10.1016/j.nhres.2023.04.003.

[5] European Commission. Commission report on forest fires: climate change is more noticeable every year. Brussels: European Commission; 2021. https://ec.europa.eu/commission/presscorner/detail/en/ip_21_5627.

[6] Jacome Felix Oom D, De Rigo D, Pfeiffer H, Branco A, Ferrari D, Grecchi R, et al. Pan-European wildfire risk assessment. Luxembourg: Publications Office of the European Union; 2022. https://publications.jrc.ec.europa.eu/repository/handle/JRC130136.

[7] Disaster risk assessment of montenegro. Podgorica: Ministry of Interior of Montenegro; 2022. https://media.gov.me/media/gov/2021/mup/nacionalna-procjena-rizika-elektronska-publikacija.pdf.

[8] Hysa A, Spalevic V, Dudic B, Roșca S, Kuriqi A, Bilașco Ș, et al. Utilizing the available open-source remotely sensed data in assessing the wildfire ignition and spread capacities of vegetated surfaces in Romania. Remote Sens. 2021;13(14):2737. doi: 10.3390/rs13142737.

[9] Xie H, Yao G, Liu G. Spatial evaluation of the ecological importance based on GIS for environmental management: a case study in Xingguo county of China. Ecol Indic. 2015;51:3–12. doi: http://dx.doi.org/10.1016/j.ecolind.2014.08.042.

[10] Valjarević A, Filipović D, Valjarević D, Milanović M, Milošević S, Živić N, et al. GIS and remote sensing techniques for the estimation of dew volume in the Republic of Serbia. Meteorolog Appl. 2020;27(3):1930. doi: 10.1002/met.1930.

[11] Marić I, Šiljeg A, Cukrov N, Roland V, Domazetović F. How fast does tufa grow? Very high-resolution measurement of the tufa growth rate on artificial substrates by the development of a contactless image-based modelling device. Earth Surf Process Landf. 2020;45(10):2331–49. doi: 10.1002/esp.4883.

[12] Domazetović F, Šiljeg A, Lončar N, Marić I. Development of automated multicriteria GIS analysis of gully erosion susceptibility. Appl Geogr. 2019;112:102083. doi: 10.1016/j.apgeog.2019.102083.

[13] Micić Ponjiger T, Lukić T, Wilby RL, Marković SB, Valjarević A, Dragićević S, et al. Evaluation of rainfall erosivity in the western balkans by mapping and clustering ERA5 reanalysis data. Atmosphere. 2023;14(1):104. doi: 10.3390/atmos14010104.

[14] Vujačić D, Milevski I, Mijanović D, Vujović F, Lukić TI. nitial results of comparative assessment of soil erosion intensity using the WIntErO model: a case study of polimlje and shirindareh drainage basins. Carpathian J Earth Environ Sci. 2023;18(2):385–404. doi: 10.26471/cjees/2023/018/267.

[15] Valjarević A, Milanović M, Gultepe I, Filipović D, Lukić T. Updated Trewartha climate classification with four climate change scenarios. Geograph J. 2022;188(4):506–17. doi: 10.1111/geoj.12458.

[16] Šiljeg A, Marić I, Krekman S, Cukrov N, Lovrić M, Domazetović F, et al. Mapping of marine litter on the seafloor using WASSP S3 multibeam echo sounder and Chasing M2 ROV. Front Earth Sci. 2023;11:1133751. doi: 10.3389/feart.2023.1133751.

[17] Yalew SG, Van Griensven A, van der Zaag P. AgriSuit: a web-based GISMCDA framework for agricultural land suitability assessment. Comput Electron Agric. 2016;128:1–8. doi: 10.1016/j.compag.2016.08.008.

[18] Takam Tiamgne X, Kanungwe Kalaba F, Raphael Nyirenda V, Phiri D. Modelling areas for sustainable forest management in a mining and human dominated landscape: a geographical information system (GIS)-multi-criteria decision analysis (MCDA) approach. Ann GIS. 2022;28(3):343–57. doi: 10.1080/19475683.2022.2026469.

[19] Gigović L, Jakovljević G, Sekulović D, Regodić M. GIS multi-criteria analysis for identifying and mapping forest fire hazard: Nevesinje, Bosnia and Herzegovina. Tehnički Vjesn. 2018;25(3):891–7. doi: 10.17559/TV-20151230211722.
[20] Milanović S, Trailović Z, Milanović SD, Hochbichler E, Kirisits T, Immitzer M, et al. Country-level modeling of forest fires in austria and the czech republic: insights from open-source data. Sustainability. 2023;15:5269. doi: 10.3390/su15065269.
[21] Durlević U, Novković I, Lukić T, Valjarević A, Samardžić I, Krstić F, et al. Multihazard susceptibility assessment: a case study—Municipality of Štrpce (Southern Serbia). Open Geosci. 2021;13:1414–31. doi: 10.1515/geo-2020-0314.
[22] Alonso-Benito A, Arroyo LA, Arbelo M, Hernández-Leal P. Fusion of WorldView-2 and LiDAR data to map fuel types in the Canary Islands. Remote Sens. 2016;8(8):669. doi: 10.3390/rs8080669.
[23] Novo A, Fariñas-Álvarez N, Martínez-Sánchez J, González-Jorge H, Fernández Alonso JM, Lorenzo H. Mapping forest fire risk—a case study in Galicia (Spain). Remote Sens. 2020;12(22):3705. doi: 10.3390/rs12223705.
[24] Marić I, Šiljeg A, Domazetović F. Derivation of wildfire ignition index using GIS-MCDA from high-resolution UAV imagery data and perception analysis in settlement Sali, Dugi Otok Island (Croatia). 7th International Conference on Geographical Information Systems Theory, Applications and Management – GISTAM; 2021. p. 90–7. doi: 10.5220/0010465000900097.
[25] Liao J, Zhou J, Yang W. Comparing LiDAR and SfM digital surface models for three land cover types. Open Geosci. 2021;13(1):497–504. doi: 10.1515/geo-2020-0257.
[26] Chuvieco E, Congalton RG. Application of remote sensing and geographic information systems to forest fire hazard mapping. Remote Sens Environ. 1989;29(2):147–59. doi: 10.1016/0034-4257(89)90023-0.
[27] Setiawan I, Mahmud AR, Mansor S, Mohamed Shariff AR, Nuruddin AA. GIS-grid-based and multi-criteria analysis for identifying and mapping peat swamp forest fire hazard in Pahang, Malaysia. Disaster Prev Manag: An Int J. 2004;13(5):379–86. doi: 10.1108/09653560410568507.
[28] Akbulak C, Tatlı H, Aygün G, Sağlam B. Forest fire risk analysis via integration of GIS, RS and AHP: The Case of Çanakkale, Turkey. J Hum Sci. 2018;15(4):2127–43. doi: 10.14687/jhs.v15i4.5491.
[29] Akay AE, Şahin H. Forest fire risk mapping by using GIS techniques and AHP method: a case study in Bodrum (Turkey. Eur J For Eng. 2019;5(1):25–35. doi: 10.33904/ejfe.579075.
[30] Van Hoang T, Chou TY, Fang YM, Nguyen NT, Nguyen QH, Xuan Canh P, et al. Mapping forest fire risk and development of early warning system for NW Vietnam using AHP and MCA/GIS methods. Appl Sci. 2020;10(12):4348. doi: 10.3390/app10124348.
[31] Sinha A, Nikhil S, Ajin RS, Danumah JH, Saha S, Costache R, et al. Wildfire risk zone mapping in contrasting climatic conditions: an approach employing AHP and F-AHP models. Fire. 2023;6(2):44. doi: 10.3390/fire6020044.
[32] Nikolić G, Vujović F, Golijanin J, Šiljeg A, Valjarević A. Modelling of wildfire susceptibility in different climate zones in montenegro using GIS-MCDA. Atmosphere. 2023;14(6):929. doi: 10.3390/atmos14060929.
[33] Kant Sharma L, Kanga S, Singh Nathawat M, Sinha S, Chandra Pandey P. Fuzzy AHP for forest fire risk modeling. Disaster Prev Manag: An Int J. 2012;21(2):160–71. doi: 10.1108/09653561211219964.
[34] Eskandari S, Miesel JR. Comparison of the fuzzy AHP method, the spatial correlation method, and the Dong model to predict the fire high-risk areas in Hyrcanian forests of Iran. Geomatics Nat Hazards Risk. 2017;8(2):933–49. doi: 10.1080/19475705.2017.1289249.
[35] Kumi-Boateng B, Peprah MS, Larbi EK. Prioritization of forest fire hazard risk simulation using hybrid grey relativity analysis (HGRA) and fuzzy analytical hierarchy process (FAHP) coupled with multi-criteria decision analysis (MCDA) techniques–a comparative study analysis. Geodesy Cartogr. 2021;47(3):147–61. doi: 10.3846/gac.2021.13028.
[36] Tiwari A, Shoab M, Dixit A. GIS-based forest fire susceptibility modeling in Pauri Garhwal, India: a comparative assessment of frequency ratio, analytic hierarchy process and fuzzy modeling techniques. Nat Hazards. 2021;105:1189–230.
[37] Abdo HG, Almohamad H, Al Dughairi AA, Al-Mutiry M. GIS-based frequency ratio and analytic hierarchy process for forest fire susceptibility mapping in the western region of Syria. Sustainability. 2022;14(8):4668. doi: 10.3390/su14084668.
[38] Pradeep GS, Danumah JH, Nikhil S, Prasad MK, Patel N, Mammen PC, et al. Forest fire risk zone mapping of Eravikulam National Park in India: a comparison between frequency ratio and analytic hierarchy process methods. Croatian J Eng: J Theory Appl For Eng. 2022;43(1):199–217. doi: 10.5552/crojfe.2022.1137.
[39] Arca D, Hacısalihoğlu M, Kutoğlu ŞH. Producing forest fire susceptibility map via multi-criteria decision analysis and frequency ratio methods. Nat Hazards. 2020;104:73–89. doi: 10.1007/s11069-020-04158-7.
[40] Tehrany MS, Özener H, Kalantar B, Ueda N, Habibi MR, Shabani F, et al. Application of an ensemble statistical approach in spatial predictions of bushfire probability and risk mapping. J Sens. 2021;2021:1–31. doi: 10.1155/2021/6638241.
[41] Pourtaghi ZS, Pourghasemi HR, Rossi M. Forest fire susceptibility mapping in the Minudasht forests, Golestan province, Iran. Environ Earth Sci. 2015;73(4):1515–33. doi: 10.1007/s12665-014-3502-4.
[42] Mohammed OA, Vafaei S, Kurdalivand MM, Rasooli S, Yao C, Hu T. A comparative study of forest fire mapping using GIS-based data mining approaches in Western Iran. Sustainability. 2022;14(20):13625. doi: 10.3390/su142013625.
[43] Salavati G, Saniei E, Ghaderpour E, Hassan QK. Wildfire risk forecasting using weights of evidence and statistical index models. Sustainability. 2022;14(7):3881. doi: 10.3390/su14073881.
[44] Regmi AD, Devkota KC, Yoshida K, Pradhan B, Pourghasemi HR, Kumamoto T, et al. Application of frequency ratio, statistical index, and weights-of-evidence models and their comparison in landslide susceptibility mapping in Central Nepal Himalaya. Arab J Geosci. 2014;7:725–42. doi: 10.1007/s12517-012-0807-z.
[45] Abedi Gheshlaghi H, Feizizadeh B, Blaschke T. GIS-based forest fire risk mapping using the analytical network process and fuzzy logic. J Environ Plan Manag. 2020;63(3):481–99. doi: 10.1080/09640568.2019.1594726.
[46] Erdin C, Çağlar M. Rural fire risk assessment in gis environment using fuzzy logic and the AHP approaches. Pol J Environ Stud. 2021;30(6):4971–84. doi: 10.15244/pjoes/136009.
[47] Zhang F, Zhang B, Luo J, Liu H, Deng Q, Wang L, et al. Forest fire driving factors and fire risk zoning based on an optimal parameter logistic regression model: a case study of the Liangshan Yi Autonomous Prefecture, China. Fire. 2023;6(9):336. doi: 10.3390/fire6090336.
[48] Chang Y, Zhu Z, Bu R, Chen H, Feng Y, Li Y, et al. Predicting fire occurrence patterns with logistic regression in Heilongjiang

Province, China. Landsc Ecol. 2013;28:1989–2004. doi: 10.1007/s10980-013-9935-4.
[49] Milanović S, Marković N, Pamučar D, Gigović L, Kostić P, Milanović SD. Forest fire probability mapping in eastern Serbia: Logistic regression versus random forest method. Forests. 2020;12(1):5. doi: 10.3390/f12010005.
[50] Su Z, Hu H, Wang G, Ma Y, Yang X, Guo F. Using GIS and Random Forests to identify fire drivers in a forest city, Yichun, China. Geomatics, Nat Hazards Risk. 2018;9(1):1207–29. doi: 10.1080/19475705.2018.1505667.
[51] Iban MC, Sekertekin A. Machine learning based wildfire susceptibility mapping using remotely sensed fire data and GIS: A case study of Adana and Mersin provinces, Turkey. Ecol Inform. 2022;69:101647. doi: 10.1016/j.ecoinf.2022.101647.
[52] Trucchia A, Meschi G, Fiorucci P, Provenzale A, Tonini M, Pernice U. Wildfire hazard mapping in the eastern Mediterranean landscape. Int J Wildland Fire. 2023;32(3):417–34. doi: 10.1071/WF22138.
[53] Sevinç V. Mapping the forest fire risk zones using artificial intelligence with risk factors data. Environ Sci Pollut Res. 2023;30(2):4721–32. doi: 10.1007/s11356-022-22515-w.
[54] Sari F. Assessment of the effects of different variable weights on wildfire susceptibility. Eur J For Res. 2024;143:651–70. doi: 10.1007/s10342-023-01643-z.
[55] Trucchia A, Meschi G, Fiorucci P, Gollini A, Negro D. Defining wildfire susceptibility maps in Italy for understanding seasonal wildfire regimes at the national level. Fire. 2022;5(1):30. doi: 10.3390/fire5010030.
[56] Hysa A, Spalevic V. Testing NDVI, tree cover density and land cover type as fuel indicators in the wildfire spread capacity index (WSCI): case of Montenegro. Not Botanicae Horti Agrobotanici Cluj-Napoca. 2020;48(4):2368–84. doi: 10.15835/nbha48411993.
[57] Vujović F, Izrada GIS. modela za kartiranje hazarda od šumskog požara. MSc thesis. Univerzitet Crne Gore, Filozofski fakultet; 2022. https://www.ucg.ac.me/skladiste/blog_1277/objava_153302/fajlovi/Filip%20Vujovi%C4%87%20-%20IZRADA%20GIS%20MODELA%20ZA%20KRATIRANJE%20HAZARDA%20OD%20%C5%A0UMSKOG.pdf.
[58] Božović D, Knežević M, Aleksić M, Iker O, Gostimirović L. Forest fire risk management information systems in Montenegro. Agric Forestry/Poljoprivreda i Šumarstvo. 2022;68(2):65–81. doi: 10.17707/AgricultForest.68.2.05.
[59] MONSTAT. Statistical Yearbook, 2023. https://www.monstat.org/uploads/files/publikacije/GODISNJAK%202023.pdf.
[60] Nikolić G, Vujović F, Grozdanić G, Valjarević A. Geomorphological Characteristics of Montenegro. In: Barović G, editor. Speleology of Montenegro. Cham: Springer. https://link.springer.com/book/9783031493744.
[61] Frankl A, Lenaerts T, Radusinović S, Spalevic V, Nyssen J. The regional geomorphology of Montenegro mapped using land surface parameters. Z Geomorphol. 2016;60(1):21–34. doi: 10.1127/zfg/2016/0221.
[62] Burić M, Micev B, Mitrović L. Climate atlas of montenegro. Podgorica, Montenegro: Montenegrin academy of sciences and art; 2012. https://canupub.me/knjiga/atlas-klime-crne-gore/.
[63] Ministry of Agriculture and Rural Development of Montenegro. The First National Forest Inventory of Montenegro—Final Report, 2013. https://www.researchgate.net/publication/296561640_The_First_National_Forest_Inventory_of_Montenegro_-_Final_Report.
[64] Stavi I. Wildfires in grasslands and shrublands: A review of impacts on vegetation, soil, hydrology, and geomorphology. Water. 2019;11(5):1042. doi: 10.3390/w11051042.
[65] Dragićević S, Filipović D. Natural Conditions and Disasters in Planning and Protection of Space. Belgrade, Serbia: University of Belgrade-Faculty of Geography; 2016.
[66] Büttner G, Kosztra B, Soukup T, Sousa A, Langanke T. CLC2018 technical guidelines. Copenhagen: European Environment Agency; 2017. https://land.copernicus.eu/en/technical-library/clc-2018-technical-guidelines/@@download/file.
[67] Povak NA, Hessburg PF, Salter RB. Evidence for scale-dependent topographic controls on wildfire spread. Ecosphere. 2018;9(10):e02443. doi: 10.1002/ecs2.2443.
[68] European Environmental Protection Agency. Available online: https://sdi.eea.europa.eu/catalogue/srv/api/records/3473589f-0854-4601-919e-2e7dd172ff50 (accessed on 10 March 2024).
[69] Mouratidis A, Ampatzidis D. European digital elevation model validation against extensive global navigation satellite systems data and comparison with SRTM DEM and ASTER GDEM in Central Macedonia (Greece). ISPRS Int J Geo-Inform. 2019;8(3):108. doi: 10.3390/ijgi8030108.
[70] Köppen W. Die Wärmezonen der Erde, nach der Dauer der heissen, gemässigten und kalten Zeit und nach der Wirkung der Wärme auf die organische Welt betrachtet. Meteorol Z. 1884;1(21):5–226.
[71] MONSTAT. Available online: https://www.monstat.org/userfiles/file/Metodologija%20statisti%C4%8Dkog%20teritorijalnog%20registra.pdf (accessed on 10 March 2024).
[72] Giglio L, Schroeder W, Justice CO. The collection 6 MODIS active fire detection algorithm and fire products. Remote Sens Environ. 2016;178:31–41. doi: 10.1016/j.rse.2016.02.054.
[73] Domazetović F, Šiljeg A, Lončar N, Marić I. GIS automated multi-criteria analysis (GAMA) method for susceptibility modelling. Methods X. 2019;6:2553–661. doi: 10.1016/j.mex.2019.10.031.
[74] Ramík J, Korviny P. Inconsistency of pair-wise comparison matrix with fuzzy elements based on geometric mean. Fuzzy Sets Syst. 2010;161(11):1604–13. doi: 10.1016/j.fss.2009.10.011.
[75] Holecek P, Talašová J. A free software tool implementing the fuzzy AHP method. In: Proceedings 34th Internation Conference of Mathmatical Methods in Economics; 2016. p. 266–71.
[76] Eastman JR. Multi-criteria evaluation and GIS. Geographical Inf Syst. 1999;1(1):493–502.
[77] Youssef B, Bouskri I, Brahim B, Kader S, Brahim I, Abdelkrim B, et al. The contribution of the frequency ratio model and the prediction rate for the analysis of landslide risk in the Tizi N'tichka area on the national road (RN9) linking Marrakech and Ouarzazate. Catena. 2023;232:107464. doi: 10.1016/j.catena.2023.107464.
[78] de Santana RO, Delgado RC, Schiavetti A. Modeling susceptibility to forest fires in the Central Corridor of the Atlantic Forest using the frequency ratio method. J Environ Manag. 2021;296:113343. doi: 10.1016/j.jenvman.2021.113343.
[79] Fangyu LI, Hua HE. Assessing the accuracy of diagnostic tests. Shanghai Arch Psychiatry. 2018;30(3):207. doi: 10.11919%2Fj.issn.1002-0829.218052.
[80] Carnicer J, Alegria A, Giannakopoulos C, Di Giuseppe F, Karali A, Koutsias N, et al. Global warming is shifting the relationships between fire weather and realized fire-induced CO2 emissions in Europe. Sci Rep. 2022;12(1):10365. doi: 10.1038/s41598-022-14480-8.
[81] Kreider MR, Higuera PE, Parks SA, Rice WL, White N, Larson AJ. Fire suppression makes wildfires more severe and accentuates impacts

of climate change and fuel accumulation. Nat Commun. 2024;15(1):2412. doi: 10.1038/s41467-024-46702-0.

[82] Rouet-Leduc J, Pe'er G, Moreira F, Bonn A, Helmer W, Shahsavan Zadeh SA, et al. Effects of large herbivores on fire regimes and wildfire mitigation. J Appl Ecol. 2021;58(12):2690–702. doi: 10.1111/1365-2664.13972.

[83] Zeleke WM, Wildfire Hazard Mapping using GIS-MCDA and Frequency Ratio Models: A Case Study in Eight Counties of Norway. MSc thesis, University of Gävle, 2019, https://www.diva-portal.org/smash/record.jsf?pid=diva2%3A1382747&dswid=-6013.

[84] Salma, Nikhil S, Danumah JH, Prasad MK, Nazar N, Saha S, et al. Prediction capability of the MCDA-AHP model in wildfire risk zonation of a protected area in the Southern Western Ghats. Environ Sustainability. 2023;6(1):59–72. doi: 10.1007/s42398-022-00259-0.